Pergamon

Available online at www.sciencedirect.com
SCIENCE DIRECT®

Cement and Concrete Research 33 (2003) 1567–1574

CEMENT AND CONCRETE RESEARCH

Effect of geothermal waste on strength and microstructure of alkali-activated slag cement mortars

J.I. Escalante-García*, A.V. Gorokhovsky, G. Mendoza, A.F. Fuentes

Centro de Investigación y de Estudios Avanzados (Cinvestav-Saltillo), PO BOX 663, Saltillo, Coahuila, CP 25000, Mexico

Received 10 October 2001; accepted 26 March 2003

Abstract

Mortars of blast furnace slag replaced with 10% of a geothermal silica waste were cured for 90 days. The binder was activated by 6 wt.% Na_2O equivalent of NaOH and water glass. The presence of the silica enhanced the formation of hydration products as shown by nonevaporable water (NEW) results. Backscattered electron images indicated that the microstructures of blended slag had less porosity than those of neat slag mortars and the interfacial zone between aggregate and hydration products was dense and of homogeneous composition similar to the matrix of hydration products. The main hydration products were C-S-H and for NaOH a hydrotalcite type phase was found as finely intermixed with the C-S-H.

Keywords: Microstructure; EDX; Mechanical properties; Alkali-activated cement; Geothermal silica waste

1. Introduction

Blast furnace slag has been used in combination with Portland cement, as aggregate or cementive fraction; improving the characteristics of Portland cement [1]. Binders based on alkali activated are of interest due to their properties in comparison to Portland cement—fast development and higher levels of mechanical strength, better durability, etc. [2–5]. Many papers concentrate on different variables that affect the properties of activated slags, e.g., the effect of the activating agents on the hydration products and mechanical properties [6–8] and microstructures [2,9,10]. However, there is a reduced number of reports on the use of other by-products in combination with activated blast furnace slags [11–14] or with Portland cement [15,16]. One by-product with potential as a cementitious additive is the geothermal silica waste (GSW) that originates from the electricity generation from geothermal resources, which are available worldwide. GSW is similar to microsilica: it has high SiO_2 content and very high surface area. Detailed information regarding the origin and treatment of the GSW was provided and discussed elsewhere [17,18]; additionally, its pozzolanic behavior is under study in blends with Portland cement [19].

Microsilica and other fine-sized materials are added to Portland cement to increase strength by means of the microfiller effect and its pozzolanic behavior, to improve durability [20] and mechanical strength by reducing the porosity of the hydration products formed in the interfacial zone hcp-aggregate [8,21,22]. Inert and hydraulic admixtures can accelerate the hydration reactions in Portland cement [23–26] as they are potential sites for heterogeneous nucleation of hydration products, improving mechanical strength. Ultrafine materials have also been used in the activation of slags to improve mechanical properties [12,13].

This work concentrated on mortars with a binder, activated by sodium hydroxide and waterglass, formed by blast furnace slag partially replaced by a GSW. The report includes results from the reactivity of the systems, elemental distribution in the hydration products and interfacial characteristics; for the activation with NaOH, some results are presented for the composition of the hydration products formed.

2. Experimentation

2.1. Materials and mortars preparation

The granulated slag was supplied and sampled at the Cementos Apasco Plant (Ramos Arizpe, Mexico). A pilot ball mill was used to prepare the slag to Blaine surface areas

---

* Corresponding author.
E-mail address: jieg@saltillo.cinvestav.mx (J.I. Escalante-García).

0008-8846/03/$ – see front matter © 2003 Elsevier Ltd. All rights reserved.
doi:10.1016/S0008-8846(03)00133-9

of 450 m^2/kg (B1) and 350 m^2/kg (B2). The GSW was obtained from the Cerro Prieto plant of the Mexican Federal Electricity (CFE). One ordinary Portland cement (Cementos Apasco, Ramos Arizpe plant) was employed for comparative purposes. Table 1 gives the chemical composition of the slag and GSW.

Mortars were prepared at binder/sand ratio of 1:2.78 using standard Ottawa sand. The activating agents were technical grade NaOH and waterglass ($SiO_2/Na_2O \approx 2$) added in equivalent 6% Na_2O with respect to the weight of the binder. Lime was added to all mixes as an activating agent at 4 wt.% of the binder. The dry powders of slag and GSW were mixed in the laboratory, the latter replaced the slag at 0% and 10% in weight The water/binder ratios used were 0.35 and 0.45 for activation with NaOH and waterglass, respectively, to obtain a good consistency. Due to the very high surface area of the silica (about 20,000 m^2/kg [17]), a Superplasticizer Rehobuild 1000 was added to the mortars with GSW to maintain good consistency by keeping constant the water/binder ratios. Mix details are shown in Table 2.

Batches of 10 kg were mixed in a laboratory blender for 4 min. Mortar cubes of 50 mm were cast in molds made of a nylon highly resistant to alkali attack. The molds were covered with a damp cloth and a plastic foil, to reduce moisture losses, and kept in a high humidity room for 24 h at 20 ± 2 °C. After demolding, the cubes were submerged in water at 20 ± 2 °C, from this point time started to count for characterization at different ages.

2.2. Characterization

Compressive strength was evaluated from 1 to 90 days, the average of four cubes is reported. Fragments from mechanical testing were dried in vacuum at 105 °C for 12 h to eliminate the free water available for the reactions. Nonevaporable water (NEW) was used as a measure of the degree of reaction of the various cements prepared. From each sample, a few lumps of material (≅30 g) were weighed (precision 0.0001 g) after drying at 130 °C and after ignition at 950 °C, the NEW was estimated by the formula $NEW = 100 \times (weight_{130\ °C} - weight_{950\ °C})/(0.2642 \times weight_{950\ °C})$. The factor of 0.2642 was introduced to correct for the effect of the sand weight and to refer NEW only to the cementive material.

Table 1
Chemical composition of starting materials

Oxide	Slag	Silica
SiO_2	31.6	95.2
Al_2O_3	9.67	–
CaO	34.59	0.98
Fe_2O_3	4.81	1.00
MgO	10.14	0.231
MnO	0.84	–
K_2O	0.90	1.03
Na_2O	0.94	0.91
SO_3	5.18	0.02
Cl	–	0.20

Table 2
Blending proportions and compositions of the mortars prepared with slag

Water/solids	Waterglass		NaOH		
	0.45		0.35		
Slag (%)	100	90	100	90	90[a]
Silica (%)	0	10	0	10	10
Plasticizer (%)	0	1	0	2	2
Na_2O (%) equivalent[b]	6		6		
CH (%)	4[b]		4[b]		
B1 blaine 450 m^2/kg, B2 blaine 350 m^2/kg					

[a] Only this was mixed with blaine B2, all others with blaine B1.

[b] With respect to the weight of slag + silica.

Samples of 90 days old were used for characterization by scanning electron microscopy (SEM). The specimens were mounted in resin, ground and polished using diamond pastes down to 1/4 μm with an oil-based lubricant. Further carbon coating was necessary to make the samples conductive under the electronic microscope (Jeol 6300) equipped with Backscattered electron imaging (BEI) and EDS analysis.

3. Results and discussion

3.1. Reactivity and compressive strength

Table 3 presents the results of NEW. For both systems, the presence of the GSW enhanced the reactivity of the slag for the Blaine B1. The GSW could be performing as heterogeneous nucleation centers for the precipitation of the hydration products after the dissolution of the slag grains under the alkali action. From the lime/silica ratio of 0.4, higher than that used in a study of pozzolanic materials of 0.25 [27], it is possible to expect a pozzolanic behavior of the silica with the lime, the latter is also an activant to the slag. For mortar with slag B2 and 10% silica activated by NaOH, the NEW values were lower than those of corresponding neat slag B1. This indicates that the mechanical activation of milling to lower Blaine B2 (larger particle size) was insufficient to promote activation of the slag. Even in the presence of the GSW, the slag reactivity was lower than that of the neat slag B1.

Table 3
Non evaporable water results for activated slags, data in % with respect to the calcined weight of the sample

	% Silica replacement	Curing days					
		1	3	7	14	28	90
Slag + NaOH	0	6.0	7.1	7.8	8.4	8.8	9.9
	10	7.0	8.5	9.0	9.1	9.4	10.8
	10[a]	5.6	5.9	7.0	7.6	8.4	9.1
Slag + Waterglass	0	5.8	6.3	7.1	8.2	9.4	11.4
	10	9.7	10.7	10.8	11.5	12	13.2

[a] Data for slag of blaine B2 350 m^2/kg, all other data for slag of blaine B1 450 m^2/kg.

Table 4
Compressive strength of the activated slags

	% silica	Curing days					
		1	3	7	14	28	90
OPC mortar	0	26.2	31.6	35.6	36.4	37.8	44.2
		(3.6)	(1.7)	(2.5)	(8.0)	(2.6)	(5.2)
Slag + NaOH	0	15.9	19.3	21.4	28.7	29.8	38.4
		(1.6)	(2.3)	(1.8)	(1.7)	(1.7)	(2.3)
	10	22.5	26.8	30.9	37.3	39.2	43.4
		(3.0)	(2.2)	(4.6)	(4.4)	(2.0)	(2.6)
	10[a]	14.5	18.6	22.7	25.6	29.7	32.6
		(0.5)	(1.2)	(1.8)	(1.8)	(2.0)	(2.4)
Slag + Waterglass	0	9.9	23.1	36.5	45.8	46.1	57.2
		(1.9)	(2.8)	(6.4)	(7.2)	(9.3)	(7.8)
	10	20.6	26.5	31.4	33.6	35.0	50.6
		(4.3)	(1.9)	(1.9)	(6.2)	(6.0)	(2.3)

Values in MPa represent the mean of four cubes, bracketed values are the standard deviation.

[a] Data for slag of blaine B2 350 m^2/kg, all other data for slag of blaine B1450 m^2/kg.

Table 4 presents the results of mechanical testing. For the slag B1 activated by NaOH, the addition of GSW increased the compressive strength, relative to the neat slag, since the first day and up to 90 days of curing, whereas the strength of slag B2 was lower at all times. These results correlated well with the observed reactivity of this system, in that the reduced reactivity of the slag of lower surface area resulted in lower strengths. For the neat slag B1 activated by NaOH the strengths attained were lower relative to the OPC mortars, whereas in the presence of GSW the strengths were similar to the latter from 14 days onwards. In line with the lower reactivity, the slag B2 with GSW also resulted in lower strengths relative to the OPC mortar.

For the waterglass activation, the strengths of the neat slag were higher than those of the OPC from 7 days onwards, and those of the slag with GSW outvalued the latter only after 90 days. Compared to the neat slag, the presence of GSW resulted in higher strengths during the first 3 days. This situation was inverted afterwards. Even though the NEW values observed for the blended slag were higher than those of the neat slag, the compressive strength did not follow the same pattern as expected and noted with the slag activated by NaOH. The samples of blended slag activated with waterglass had many macropores of air bubbles trapped due to a fast setting during the mixing and casting stages, which reduced the strength of the mortars.

The origin of the fast setting is not clear and more work is needed to elucidate it. However, some possible mechanisms can be considered. Assuming a highly reactive GSW, considering its small particle size (agglomerates of 4 μm and particles of about 200 nm observed in SEM [19]) and its amorphous character, the chemical attack of NaOH could produce the formation of hydration products; a strong attack on PFA particles by NaOH was reported for the initial hydration periods by Shi and Day [14]. Other possibilities are also discussed in the literature [28]. A drastic increase of the viscosity of waterglass occurs if the SiO_2/Na_2O ratio is increased, which could be expected if the fine particle silica waste goes partly in solution in the early stages of mixing. On the other hand, the addition of alkali salts as NaCl, which is present in very small amounts in the GSW, to waterglass increases the viscosity and forms a gel, thought

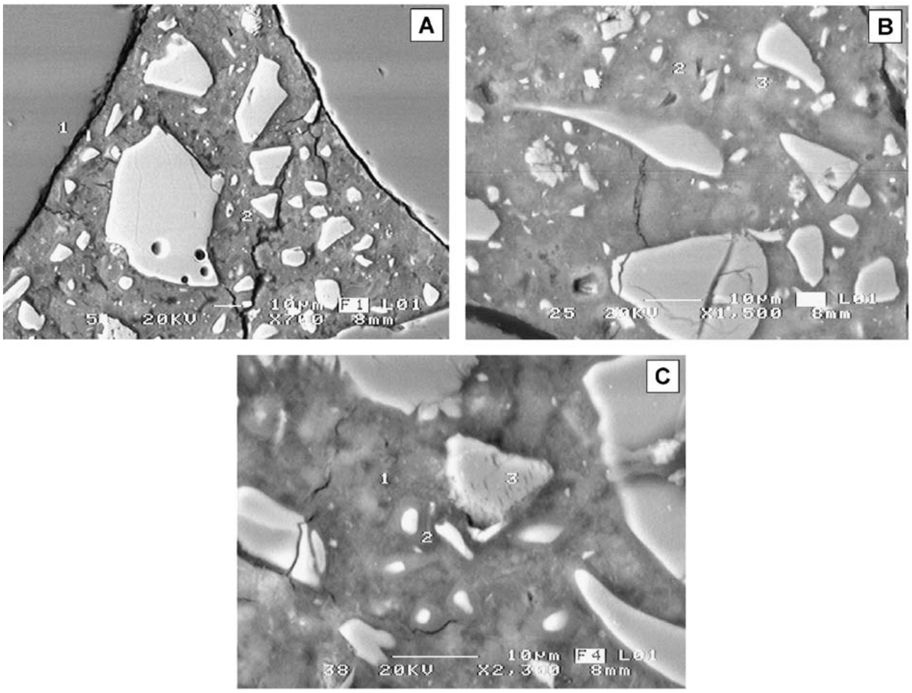

Fig. 1. SEM micrographs of NaOH-activated slag. (A) 0% silica, (B) 10% silica, blaine 450 m2/kg, (C) 10% silica, blaine 350 m^2/kg.

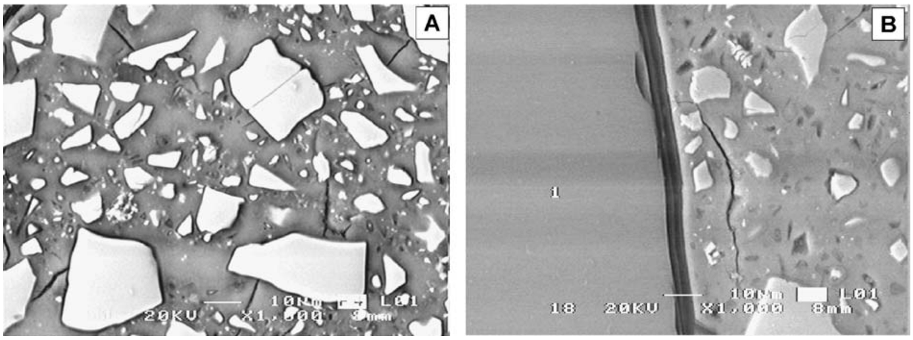

Fig. 2. SEM micrographs of waterglass slag. (A) 0% silica, (B) 10% silica.

as a result of increased intermolecular forces due to neutralization of the charge or a kind of dehydration. Also, waterglass and the GSW can react with the added lime to form C-S-H-like products. Moreover, some differences have to be considered between the slag with GSW activated first with NaOH and second with waterglass; the first could be regarded as a suspension of solid particles (slag and silica waste) in a water solution (NaOH), whereas the second is the suspension of solid particles with a sol. Thus, the second system is more prone to fast solidification; whereas for the first system, the coagulation could take place only after the transformation of the water solution to sol as a result of chemical interaction of NaOH with the silica waste and slag particles.

3.2. Microstructures and microanalysis

Fig. 1 presents the micrographs of the slags activated with NaOH. In the presence of the GSW, the matrix of hydration products appeared more compact than for the neat slag. It seems that the lower reactivity of the slag of Blaine B2 seemed to have hindered any benefit from the lower porosity in the matrix, whereas for the slag B1, the higher reactivity complemented with the improved compactness of the matrix for the higher strengths over those of the neat slag.

Fig. 2 presents the microstructures for the slag B1 activated with waterglass. The matrix of hydration products of the blended slag seems more compact and less porous than the neat slag; the latter displayed some darker areas and pores that were not noted in the presence of the GSW. Higher strength would be expected for the blended slag; however, macroporosity caused a strength reduction. The remaining slag grains looked generally smaller in the mortars with GSW relative to the neat slags, which was in line with the increased reactivity.

The microstructures of slags activated by both alkaline agents showed that the interface between the aggregates and the bulk hydration products was dense and compact, in contrast to the porous zone reported for Portland cement mortars.

Considering that NEW values indicated that the slag had actually reacted, it can be noted from Figs. 1 and 2 that for both alkalis, the predominant mechanism of

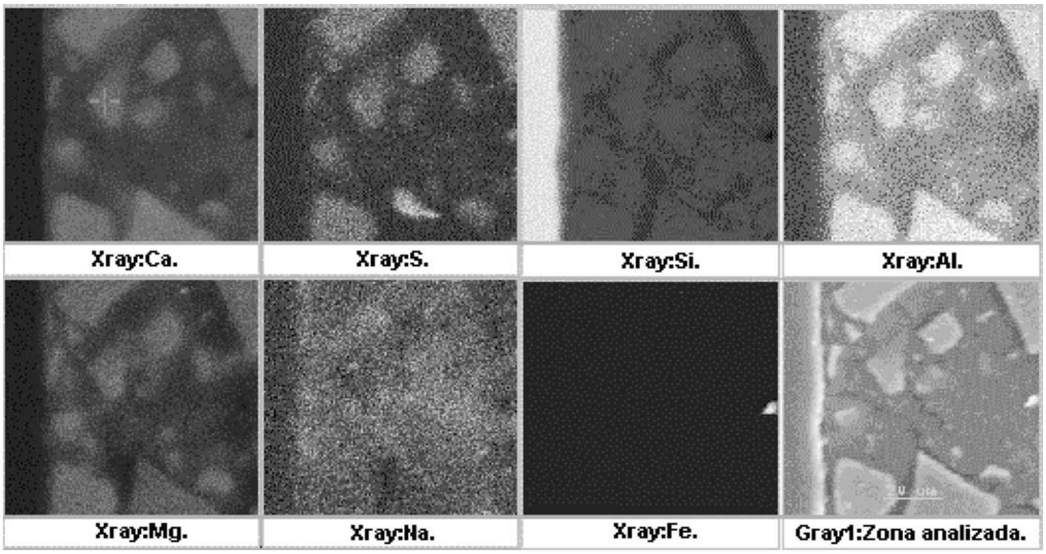

Fig. 3. X-ray elemental map of NaOH-activated slag with 0% silica.

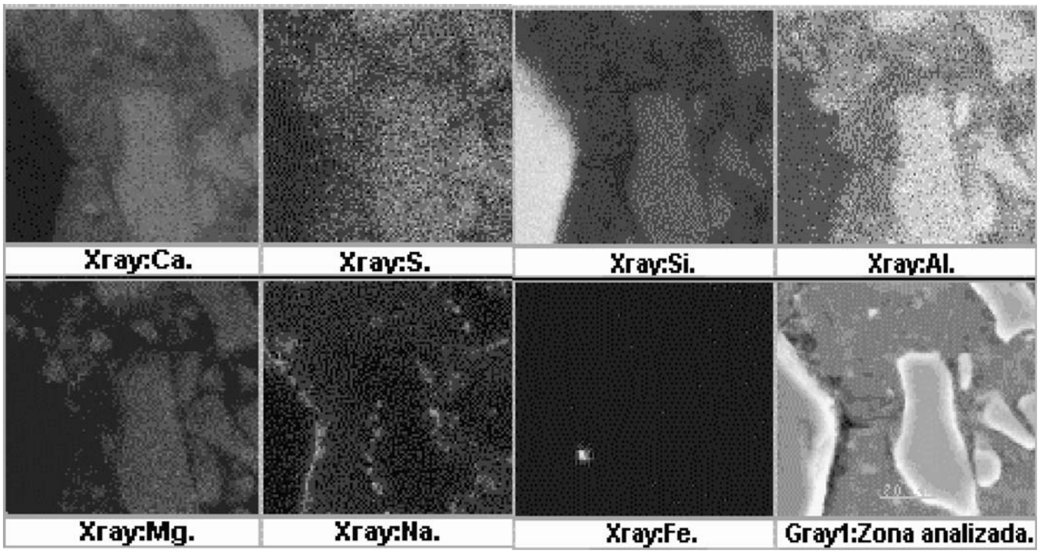

Fig. 4. X-ray elemental map of waterglass-activated slag with 0% silica.

reaction appeared to be via dissolution of the glass network and precipitation of hydration products, although some quite small slag grains reacted forming hydration products within the slag grain boundaries.

Figs. 3 and 4 present the X-ray elemental maps for the mortars of neat slags activated with NaOH and water glass. The lower right image is the photo of the analyzed area. The morphology of slag grains is angular with sharp corners and according to the slag chemical composition the main elements appearing in the maps are Ca, Si, Al, Mg and S. It can be noticed that the sodium was homogeneously distributed throughout the matrix of hydration products, although it concentrated in some areas around the slag and sand grains in the case of waterglass. The hydration products are constituted mainly by Ca, Si, Al, and Mg, which indicates the dissolution of the slag vitreous network after the alkali attack, and the precipitation of the hydration products in the spaces initially occupied by water.

Figs. 5 and 6 presents the corresponding maps for the mortars of slag with GSW activated with both alkalis. The same can be mentioned with regards to the elemental distribution in the anhydrous slag and the hydration products as well as for the Na distribution. Except for the high concentration spot of Si noted in Fig. 6, which can be attributed to a cluster of GSW or to a small sand grain, it can be said that lower contrast was noted in the Si maps, relative to Figs. 3 and 4, as a result of the higher Si concentration due to the GSW finely distributed throughout the hydration products.

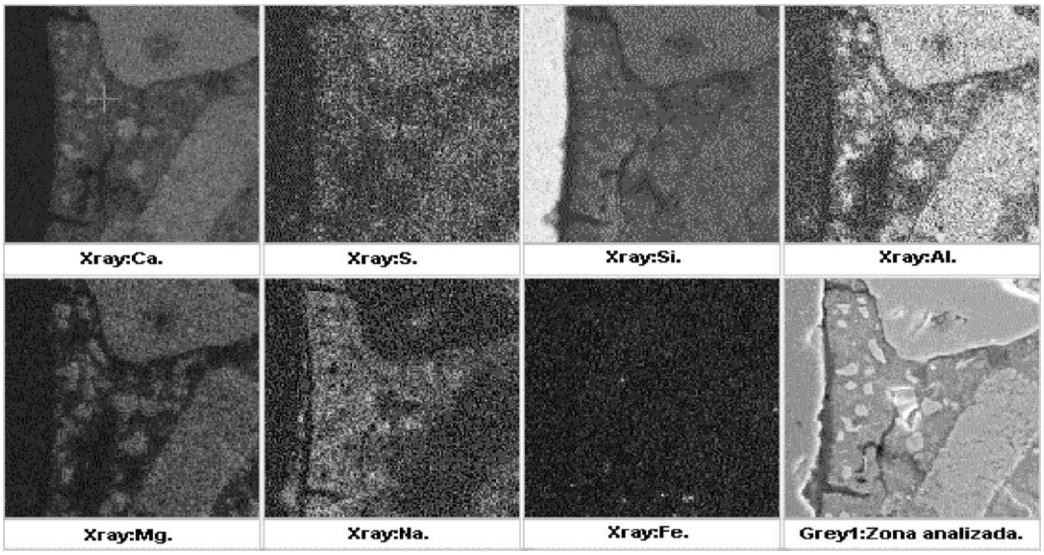

Fig. 5. X-ray elemental map of NaOH-activated slag with 10% silica.

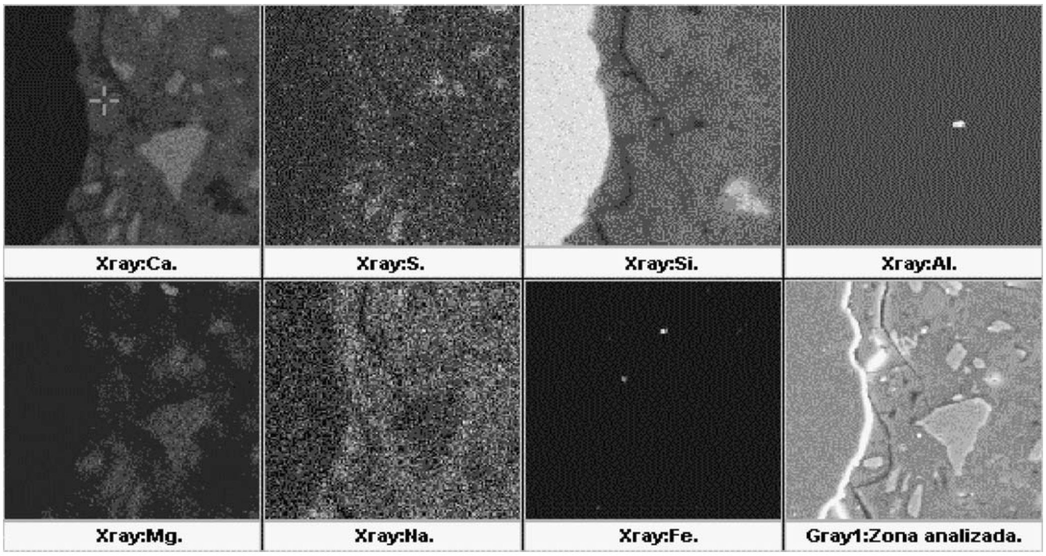

Fig. 6. X-ray elemental map of waterglass-activated slag with 10% silica.

To analyze the interfacial zone between the aggregate and hydration products, sand grains were included in the studied areas in Figs. 4–6, in all cases in the left side of the photograph. The sand grains were clearly noticeable due to the high Si concentration and the absence of any other element. As mentioned, the microstructures of all systems studied showed dense and compact interfacial zone between hydration products and aggregate. From the X-ray maps it was possible to observe that the elemental distribution was no different from the rest of the matrix of products away from the sand grains. Dense and compact interfaces were reported by Shi and Xie [29] by secondary electron images for slags activated by waterglass. The reported initially high concentrations of Si and Ca [30] from the slag dissolution (by NaOH attack), and also the possible Si dissolution from the GSW (in the appropriate cases) and the sand by the alkaline attack, can cause the condensation of SiO_4^{-4} into hydration products that will form a dense interface zone different to that formed in Portland cement mortars.

Microanalyses were carried out only for the slag activated with NaOH in order to investigate the chemical composition of the hydration products. The spot analyses were carried out randomly in the groundmass of hydration products, the results are presented in Fig. 7. The ratio Si/Ca was higher than that commonly reported for hydrated Portland cements [31,32] and was in similar range to those reported for slags activated with NaOH [2,33]. The same data in the plot of Mg/Ca vs. Al/Ca fitted a straight line with a slope that indicates a compositional ratio Mg/Al = 3.5, similar to that of the mineral hydrotalcite $Mg_6Al_2(CO3)(OH)_{16} \cdot 4H_2O$, which was also detected by X-ray diffraction. This indicates that the C-S-H in the hydration products is finely intermixed with a hydrotalcite type product. This was supported by the X-ray elemental maps, which showed a homogeneous distribution of Mg in the

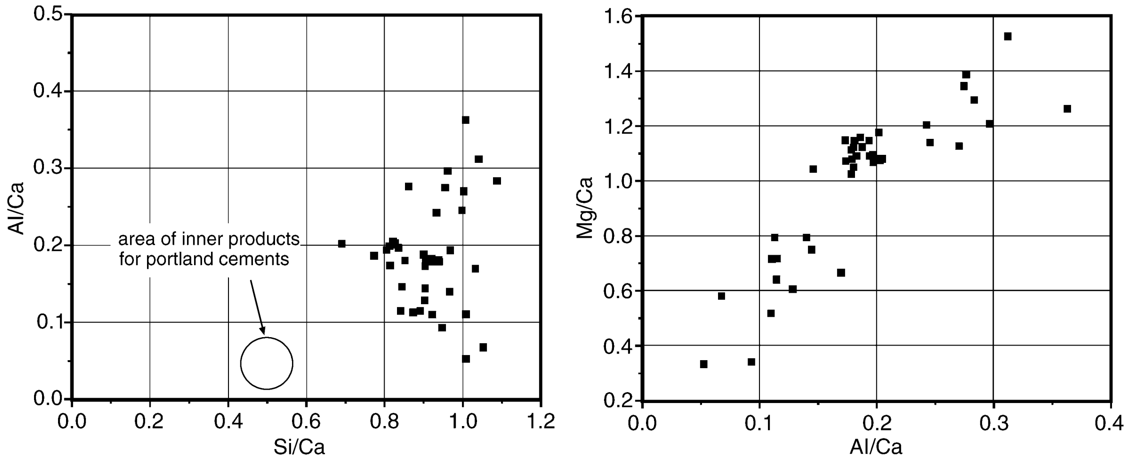

Fig. 7. Microanalysis of the hydration products of the slag hydrated with NaOH.

hydration products. No clear crystals of hydrotalcite could be resolved in the backscattered images under the microscope. Hydrotalcite was also reported for slags hydrated with NaOH and waterglass [2,33].

4. Conclusions

This work investigated the effect of the replacement of slag by 10% of GSW of very fine particle in mortars activated by NaOH and waterglass. The following conclusions can be drawn:

1. The reactivity for both slag-activated systems was increased in the presence of the silica waste; the silica particles were regarded as heterogeneous nucleation centers for the precipitation of hydration products after the dissolution of the slag.
2. The compressive strength of the slag activated by NaOH was enhanced by the presence of the silica. For the slag activated by waterglass the presence of the silica resulted in strengths reduction; this was caused by the presence of air bubbles trapped during mixing and casting of the mortars, in spite of the increased reactivity of the slag in presence of the silica. One possible reason was the excess of Si in solution with the formation of polymerized H_2SiO_3 as an inorganic binder or C-S-H-like products that caused fast setting.
3. The backscattered electron images showed that the interface of hydration products with the aggregate was dense and compact for both activated systems. The chemical composition in the interface appeared similar to the bulk of hydration products.
4. The microanalysis of the hydration products in the NaOH system indicated that in low Ca/Si C-S-H formed and was finely intermixed with a hydrotalcite like hydration product, which was confirmed by the homogeneous distribution of Mg in the matrix of hydration products.

Acknowledgements

The authors would like to thank Cementos Apasco and the Cerro Prieto plant of CFE for the materials supplied. The support of Ing. Miguel Aguilar for the operation of the microscope is gratefully acknowledged. This research was supported by the National Council of Science and Technology Conacyt Project J28273U.

References

[1] S.J. Virgalitte, M.D. Luther, J.H. Rose, B. Mather, L.W. Bell, B.A. Ehmke, P. Klieger, D.M. Roy, Ground Granulated Blast-Furnace Slag as a Cementitious Constituent in Concrete, ACI Report 233R-95, American Concrete Institute, USA, 1995, 18 pp.

[2] S.D. Wang, K.L. Scrivener, Hydration products of alkali activated slag cement, Cem. Concr. Res. 25 (1995) 561–571.

[3] C. Shi, Strength, pore structure and permeability of alkali activated slag mortars, Cem. Concr. Res. 26 (1996) 1798–1799.

[4] P.M. Gifford, J.E. Elliot, Alkali-silica reaction (ASR) and alkali carbonate reaction (ACR) in activated blast furnace slag cement (ABFSC) concrete, Cem. Concr. Res. 26 (1996) 21–26.

[5] D.M. Roy, Alkali activated cements opportunities and challenges, Cem. Concr. Res. 29 (1999) 249–254.

[6] D.M. Roy, W. Jiang, Microcharacteristics and properties of hardened alkali-activated cementitious materials, in: E.M. Carter (Ed.), Cement Technology, Ceramics Transactions, vol. 40, 1993, pp. 257–264.

[7] S.D. Wang, K.L. Scrivener, P.L. Pratt, Factors affecting the strength of alkali-activated slag, Cem. Concr. Res. 24 (1994) 1033–1043.

[8] F.G. Collins, J.G. Sanjayan, Workability and mechanical properties of alkali activated slag concrete, Cem. Concr. Res. 29 (1999) 455–459.

[9] P.J. Shilling, A. Roy, H.C. Eaton, Microstructure, strength and reaction products of ground granulated blast-furnace slag activated by highly concentrated NaOH solution, J. Mater. Res. 9 (1) (1994, Jan.) 188–197.

[10] S.N. Gosh, D.M. Joshi, S. Chanda, H. Vaishnav, Studies on activation of slag cement, in: H. Justnes (Ed.), Proceedings of the 10th International Congress on the Chemistry of Cement, 3ii092, Amarki AB and Congrex Göteborg AB, Gothemborg, Sweden, 1997, 4 pp. Gothemborg, Sweden.

[11] I. Rouseková, A. Bajza, V. Zivica, Silica fume-basic blast furnace slag systems activated by an alkali silica fume activator, Cem. Concr. Res. 27 (1997) 1825–1828.

[12] Y. Xi, D.D. Siemer, B.E. Scheetz, Strength development, hydration reaction and pore structure of autoclaved slag cement with added silica fume, Cem. Concr. Res. 27 (1997) 75–82.

[13] F. Collins, J.G. Sanjayan, Effects of ultrafine materials on workability and strength of concrete containing alkali activated slag as the binder, Cem. Concr. Res. 29 (1999) 459–462.

[14] C. Shi, R.L. Day, Early strength development and hydration of alkali activated blast furnace slag/fly ash blends, Adv. Cem. Res. 11 (1999) 189–196.

[15] S. Roy, S. Chanda, S.K. Bandopadhyay, S.N. Gosh, Investigation of Portland slag cement activated by waterglass, Cem. Concr. Res. 28 (1998) 1049–1056.

[16] T. Bakharev, J. Gnananandan Sanjayan, Y.B. Cheng, Alkali activation of Australian slag cements, Cem. Concr. Res. 29 (1999) 113–120.

[17] C. Diaz, L.M. Torres, M. Avalos-Borja, J.M. Rincon, Turning geothermal waste into glasses and glass ceramic, Am. Ceram. Soc. Bull. 72 (1993) 81–82.

[18] C. Diaz, J.M. Rincon, Tratamiento quimico de la escoria de silice de una planta geothermica para su aplicación en ceramica y vidrio, Bol. Soc. Esp. Ceram. Vidr. 29 (3) (1990) 181–184.

[19] L.Y. Gomez Zamorano, PhD thesis, Cinvestav Saltillo, 2003, in Spanish.

[20] J. Zelic, R. Krstulovic, E. Tkalcec, P. Krolo, Durability of the hydrated limestone–silica fume Portland cement mortars under sulphate attack, Cem. Concr. Res. 29 (1999) 816–819.

[21] P. Fidjestol, R. Lewis, Microsilica as an addition, in: P.C. Hewlett (Ed.), Lea's Chemistry of Cement and Concrete, Arnold, London, 1997, 675–708.

[22] S. Mindess, Interfaces in concrete, in: J.P. Skalny (Ed.), Materials Science of Concrete, vol. I, American Ceramic Society, Westerville, Ohio, USA, 1989, pp. 163–180.

[23] J.I. Escalante-García, J.H. Sharp, Effect of temperature on the hydration of the main clinker pases in Portland cements: Part II. Blended cements, Cem. Concr. Res. 28 (1998) 1259–1274.

[24] W.A. Gutterdige, J.A. Dalziel, Filler cement: the effect of the secondary component on the hydration of Portland cement: Part I. A fine non-hydraulic filler, Cem. Concr. Res. 20 (1990) 778–782.

[25] W.A. Gutterdige, J.A. Dalziel, Filler cement: the effect of the secondary component on the hydration of Portland cement: Part 2. Fine hydraulic binders, Cem. Concr. Res. 20 (1990) 853–861.

[26] A.D. Kumar, M. Roy, A study of silica fume modified cements of varied fineness, J. Am. Ceram. Soc. 67 (1) (1984) 61–64.

[27] C. Shi, R.L. Day, Pozzolanic reaction in the presence of chemical activators: Part I. Reaction kinetics, Cem. Concr. Res. 30 (2000) 51–58.

[28] Technology of Monolithic Refractories, Plibrico Japan, 1984, pp. 115–123.

[29] C. Shi, P. Xie, Interface between cement paste and quartz sand in alkali-activated slag mortars, Cem. Concr. Res. 28 (1998) 887–896.

[30] S. Song, H.M. Jennings, Pore solution chemistry of alkali activated ground granulated blast furnace slag, Cem. Concr. Res. 29 (1999) 159–170.

[31] A.M. Harrison, N.B. Winter, H.F.W. Taylor, An examination of some pure and composite Portland cement pastes using scanning electron microscopy with X-ray analytical capabilities, Proceedings of the 8th International Congress on the Chemistry of Cement, Brasil vol. IV, Abla Grafica e Editoria, Rio de Janeiro, Brazil, 1986, pp. 170–175.

[32] J.I. Escalante-García, J.H. Sharp, Variation in the composition of the C-S-H gel in Portland cement pastes cured at various temperatures, J. Am. Ceram. Soc. 82 (1999) 3237–3241.

[33] J.I. Escalante-Garcia, A.F. Fuentes, A. Gorokhovsky, P.E. Fraire-Luna, G. Mendoza-Suarez, Hydration products and reactivity of blastfurnace slag activated by various alkalis, J. Am. Ceram. Soc. (2003) (in press).